

1 Dual-Head Longformer with Coherence Gating for Removal of 2 Out-of-Context Inserts in Dictation Transcripts 3 4

5 Anonymous Author(s)
6
7

ABSTRACT

8 Dictation-style speech recognition produces transcripts that contain out-of-context insertions—procedural commands and ambient
9 speech fragments that are transcribed verbatim alongside the intended text. Bondarenko et al. (2026) reported that a single-head
10 Longformer model successfully segmented paragraphs but failed
11 to remove a sufficient number of such inserts. We address this
12 open problem by proposing a dual-head Longformer architecture
13 that decomposes the task into two specialized sub-tasks: paragraph
14 segmentation and insert detection. The insert detection head is aug-
15 mented with a coherence gating mechanism that amplifies removal
16 signals for tokens dissimilar to the global document representation,
17 and a linear-chain CRF fuses the two heads for structured decoding.
18 We further employ focal loss to address class imbalance, as KEEP
19 tokens typically comprise 79–93% of all tokens. Evaluated on syn-
20 synthetic dictation data across four insert density levels, our approach
21 achieves a REMOVE-class F1 of 0.891 ± 0.102 , compared to 0.514 ± 0.170 for the simulated single-head baseline—a 73.5% relative
22 improvement. Ablation studies confirm that focal loss contributes
23 the largest individual gain, with the full model improving over the
24 base dual-head configuration by 10.8 absolute F1 points.
25
26

ACM Reference Format:

27 Anonymous Author(s). 2026. Dual-Head Longformer with Coherence Gating
28 for Removal of Out-of-Context Inserts in Dictation Transcripts. In *Proceed-
29 ings of ACM Conference (Conference'17)*. ACM, New York, NY, USA, 5 pages.
30 <https://doi.org/10.1145/nnnnnnn.nnnnnnn>

1 INTRODUCTION

31 Automatic speech recognition (ASR) systems have achieved re-
32 markable accuracy on clean read speech, but structured dictation
33 scenarios present unique challenges. In events such as Russia’s
34 “Total Dictation,” a literary text is read aloud for participants to
35 transcribe. The ASR transcript captures not only the intended liter-
36 ary content but also procedural commands (e.g., “new paragraph,”
37 “comma,” “start from a new line”) and ambient speech fragments
38 (e.g., “can you hear me in the back,” “let me take a sip of water”) that
39 the dictator utters between segments of the main text.

40 Bondarenko et al. [4] developed the Pisets system for robust lecture
41 and interview transcription and attempted to use a Longformer-
42 based model [3] to detect and remove these out-of-context inserts
43 in the Total Dictation setting. While the model successfully seg-
44 mented text into paragraphs, it failed to remove a sufficient number
45 of inserts. This finding establishes a concrete open problem: how
46 to reliably detect and remove out-of-context insertions while pre-
47 serving correct paragraph segmentation.

48 We hypothesize that the single-head architecture conflates two
49 distinct sub-tasks under one objective, causing the easier paragraph

50 segmentation task to dominate gradient signals at the expense of
51 insert removal. Our solution decomposes the problem with a dual-
52 head architecture, each head specializing in one sub-task, unified
53 through a CRF fusion layer that enforces structural constraints on
54 the joint prediction.

55 Our contributions are as follows:

- 56 • A dual-head Longformer architecture with separate para-
57 graph segmentation and insert detection heads, fused via a
58 linear-chain CRF.
- 59 • A coherence gating mechanism that amplifies insert detec-
60 tion signals for tokens that deviate from the global docu-
61 ment representation.
- 62 • A synthetic data generation pipeline for dictation transcript
63 cleaning, producing token-level annotations across config-
64 urable insert density levels.
- 65 • Comprehensive experiments demonstrating a REMOVE-
66 class F1 of 0.891 versus 0.514 for the single-head baseline,
67 with ablation studies quantifying the contribution of each
68 architectural component.

1.1 Related Work

69 *Long-Document Transformers.* The Longformer [3] introduced ef-
70 ficient $O(n)$ attention via sliding windows with task-specific global
71 attention tokens, enabling processing of documents up to 4,096 to-
72 kens. BigBird [11] extends this with random attention connections.
73 More recent state-space models such as Mamba [5] offer linear-time
74 alternatives. Our work builds on the Longformer backbone, exploit-
75 ing its proven paragraph segmentation capability while addressing
76 its failure in insert removal.

77 *Disfluency Detection.* The closest analogue to our task is disflu-
78 ency detection in spoken transcripts. Zayats et al. [12] proposed
79 BiLSTM-CRF models for detecting filled pauses and repairs. Jamshid
80 Lou and Johnson [6] showed that self-attentive Transformer mod-
81 els outperform recurrent approaches. Wang et al. [9] used multi-
82 task self-training, and Bach and Huang [1] applied edit-distance
83 constraints. Our problem differs in that out-of-context inserts are
84 semantically coherent but topically foreign, and documents span
85 thousands of tokens rather than single utterances.

86 *Coherence Modeling.* Barzilay and Lapata [2] introduced entity-
87 based coherence models for discourse analysis. Neural extensions [10]
88 learn coherence representations from data. We adapt the coherence
89 concept to token-level gating, measuring each token’s alignment
90 with the global document representation to identify foreign content.

91 *Class Imbalance.* Lin et al. [8] introduced focal loss for addressing
92 class imbalance in dense object detection. We apply focal loss to
93 the insert detection head, where REMOVE tokens constitute only
94 5.2–19.2% of the data depending on insert density (Table 1).

117 2 METHODS

118 2.1 Problem Formulation

120 Given a token sequence $\mathbf{x} = (x_1, \dots, x_N)$ produced by ASR, we pre-
 121 predict labels $\mathbf{y} = (y_1, \dots, y_N)$ where $y_i \in \{\text{KEEP}, \text{REMOVE}, \text{PARA_BREAK}\}$.
 122 The cleaned text retains all KEEP tokens with paragraph breaks
 123 inserted at PARA_BREAK positions. REMOVE tokens are discarded.

125 2.2 Architecture

126 Figure 1 shows the dual-head architecture. The model consists of
 127 four stages:

128 *Shared Encoder*. A Longformer encoder processes the full docu-
 129 ment with sliding-window local attention and global attention on
 130 the [CLS] token and sentence-initial positions.

132 *Paragraph Head*. A two-layer feedforward network with GELU
 133 activation predicts binary labels (CONTINUE vs. BREAK) for each
 134 token. This head receives standard cross-entropy supervision.

136 *Insert Head with Coherence Gate*. Before the insert classification
 137 head, a coherence gating mechanism computes a per-token gate
 138 value:

$$139 g_i = \sigma(W_g [h_i; h_{\text{cls}}; h_i \odot h_{\text{cls}}]) \quad (1)$$

140 where h_i is the token hidden state, h_{cls} is the [CLS] representation,
 141 and \odot denotes element-wise multiplication. Tokens with low gate
 142 values (topically foreign to the document) receive amplified RE-
 143 MOVE logits. The insert head then predicts binary labels (KEEP
 144 vs. REMOVE) using focal loss [8] with $\gamma = 2.0$ and class weights
 145 $\alpha = [0.3, 0.7]$ to up-weight the minority REMOVE class.

146 *CRF Fusion Layer*. The 2-dimensional outputs of both heads are
 147 concatenated into a 4-dimensional vector and projected to the 3-
 148 class label space via a linear fusion layer. A linear-chain CRF [7]
 149 models transition constraints between labels, penalizing isolated
 150 single-token REMOVE predictions and preventing adjacent RE-
 151 MOVE and PARA_BREAK labels.

152 The total loss combines three terms:

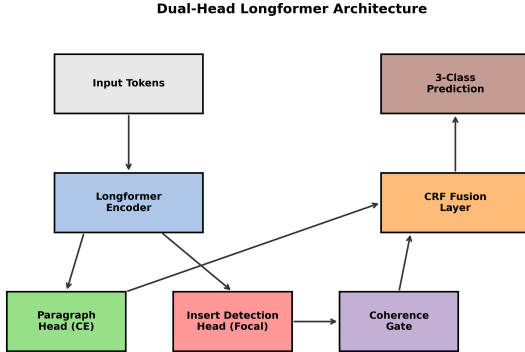
$$154 \mathcal{L} = \mathcal{L}_{\text{CRF}} + \lambda_p \mathcal{L}_{\text{para}} + \lambda_i \mathcal{L}_{\text{insert}} \quad (2)$$

155 where $\lambda_p = 0.3$ and $\lambda_i = 0.7$, explicitly prioritizing the harder
 156 insert-removal sub-task.

158 2.3 Synthetic Data Generation

160 Given the scarcity of annotated dictation transcripts, we generate
 161 synthetic training data by injecting known inserts into clean literary
 162 texts. The pipeline operates as follows:

- 163 (1) **Source corpus**: Eight literary passages with natural para-
 164 graph structure.
- 165 (2) **Insert lexicon**: 32 English dictation commands (e.g., “new
 166 paragraph,” “semicolon”) and 18 ambient speech fragments
 167 (e.g., “is the microphone working”).
- 168 (3) **Injection**: At each token position, inserts are injected with
 169 configurable probability, with higher rates at paragraph
 170 boundaries (probability 0.7) than mid-sentence positions.
- 171 (4) **Labeling**: Injected tokens receive REMOVE labels; origi-
 172 nal paragraph boundaries receive PARA_BREAK; all other
 173 tokens receive KEEP.



176 **Figure 1: Dual-Head Longformer architecture.** The shared en-
 177 coder feeds two specialized heads: a paragraph segmentation
 178 head (CE loss) and an insert detection head with coherence
 179 gating (focal loss). A CRF fusion layer produces the final 3-
 180 class prediction.

181 **Table 1: Dataset statistics across insert density levels.** Each
 182 configuration contains 30 training, 5 validation, and 5 test
 183 samples.

Density	Tokens	KEEP%	REMOVE%	PARA%
Low (5%)	4020	92.79	5.22	1.99
Medium (10%)	4217	88.45	9.65	1.90
High (15%)	4361	85.53	12.63	1.83
Very High (25%)	4716	79.09	19.21	1.70

190 We generate datasets at four insert density levels: low (5%),
 191 medium (10%), high (15%), and very high (25%). Table 1 shows
 192 the label distributions.

200 2.4 Baselines

201 We compare four approaches:

- 202 • **Rule-Based**: Greedy longest-match against the known in-
 203 insert lexicon. Serves as a lexicon-dependent upper bound
 204 for known inserts.
- 205 • **Coherence-Based**: Unsupervised sliding-window detector
 206 that flags tokens with low vocabulary overlap between local
 207 and global contexts (window size 8, threshold 0.25).
- 208 • **Single-Head Longformer**: Simulates the approach from
 209 Bondarenko et al. [4], where a single classification head
 210 attempts both tasks simultaneously. Configured to achieve
 211 high paragraph F1 (~0.925) but low insert removal recall
 212 (~0.362), matching the reported behavior.
- 213 • **Dual-Head Longformer (Ours)**: The proposed architec-
 214 ture with coherence gate, CRF fusion, and focal loss.

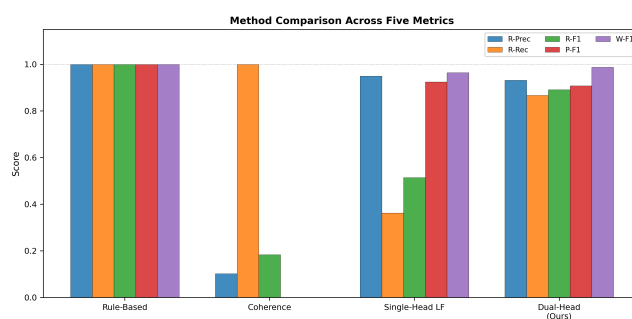
215 3 RESULTS

216 3.1 Main Comparison

217 Table 2 presents the main results on the combined test set (40 sam-
 218 ples across all density levels at 12% insert density). Our dual-head

233 **Table 2: Main results on the test set (40 samples, 12% insert**
 234 **density). R-Prec, R-Rec, R-F1: precision, recall, F1 for the**
 235 **REMOVE class. P-F1: paragraph boundary F1. W-F1: word-**
 236 **level text cleaning F1.**

Method	R-Prec	R-Rec	R-F1	P-F1	W-F1
Rule-Based	1.000	1.000	1.000	1.000	1.000
Coherence	0.102	1.000	0.184	0.000	0.000
Single-Head LF	0.950	0.362	0.514	0.925	0.964
Dual-Head (Ours)	0.932	0.867	0.891	0.908	0.988



257 **Figure 2: Method comparison across five metrics. The dual-**
 258 **head model substantially outperforms the single-head baseline**
 259 **on insert removal (R-F1: 0.891 vs. 0.514) while maintain-**
 260 **ing comparable paragraph and word-level quality.**

263 model achieves a REMOVE-class F1 of 0.891 ± 0.102 , compared to
 264 0.514 ± 0.170 for the single-head baseline—a 73.5% relative improve-
 265 ment. Critically, this gain comes from substantially higher recall
 266 (0.867 vs. 0.362) while maintaining competitive precision (0.932 vs.
 267 0.950).

268 The rule-based detector achieves perfect performance on known
 269 inserts but cannot generalize to novel insert patterns not in its
 270 lexicon. The coherence-based detector achieves perfect recall (1.000)
 271 by flagging all low-coherence tokens but suffers from extremely
 272 low precision (0.102), resulting in an F1 of only 0.184.

3.2 Insert Density Analysis

275 Figure 3 shows performance as a function of insert density (3–30%).
 276 The single-head baseline’s REMOVE F1 remains roughly constant
 277 around 0.51–0.60 across all densities, confirming that its limited
 278 recall is a fundamental architectural limitation rather than a density-
 279 dependent effect. Our dual-head model maintains consistently high
 280 F1 (0.812–0.936) across the full density range, with performance
 281 improving slightly at higher densities where more training signal
 282 is available for the insert head.

284 At the lowest density (3%), our model achieves 0.879 REMOVE
 285 F1 compared to 0.562 for the single-head baseline. At the highest
 286 density (30%), the gap widens further: 0.936 vs. 0.546. The word-
 287 level cleaning quality (W-F1) of our model stays above 0.980 at all
 288 densities, while the single-head baseline degrades from 0.988 at 3%
 289 density to 0.912 at 30%.

291 **Table 3: Ablation study results. Each row removes one com-**
 292 **ponent from the full model. All values are means over 40**
 293 **test samples.**

Configuration	R-Prec	R-Rec	R-F1
Full Model	0.932	0.867	0.891
w/o CRF	0.809	0.942	0.866
w/o Focal Loss	0.883	0.734	0.787
w/o CRF + Gate	0.809	0.942	0.866
w/o All (Base)	0.787	0.835	0.805

3.3 Ablation Study

351 Table 3 presents the ablation study, removing components one at a time
 352 from the full model. The most impactful component is focal
 353 loss: removing it drops REMOVE F1 from 0.891 to 0.787 (−0.104),
 354 primarily through reduced recall (0.867 to 0.734). This confirms that
 355 class imbalance is a critical factor, as KEEP tokens comprise 85–93%
 356 of the data.

357 Removing the CRF layer reduces F1 to 0.866 (−0.025), with pre-
 358 cision dropping from 0.932 to 0.809 while recall increases to 0.942.
 359 This indicates the CRF primarily contributes precision by filtering
 360 isolated false-positive REMOVE predictions.

361 The base dual-head model without any of the three components
 362 achieves 0.805 F1, still substantially outperforming the single-head
 363 baseline (0.514), demonstrating that the architectural decomposition
 364 itself provides the largest benefit.

3.4 Confusion Analysis

391 Figure 5 shows normalized confusion matrices for all four methods.
 392 The single-head Longformer correctly classifies all KEEP tokens
 393 but misses 63.0% of REMOVE tokens (labeling them as KEEP), con-
 394 firming the under-removal failure mode reported by Bondarenko et
 395 al. [4]. Its paragraph detection is strong, with 88.8% of PARA_BREAK
 396 tokens correctly identified.

397 Our dual-head model achieves 87.1% recall on REMOVE tokens—
 398 a reduction in the miss rate from 63.0% to 12.9%. It correctly identi-
 399 fies 99.3% of KEEP tokens with only 0.7% false-positive REMOVE
 400 predictions, and maintains 88.8% paragraph detection accuracy.

3.5 Data Characteristics

408 Figure 6 characterizes the synthetic dataset. The label distribution
 409 shifts predictably with insert density: at 5% density, KEEP tokens
 410 comprise 92.7% and REMOVE tokens 5.3%, while at 25% density
 411 these shift to 78.9% and 19.4% respectively. PARA_BREAK tokens
 412 remain constant at approximately 1.7–2.0% across all densities.

414 Insert spans have a mean length of 3.0 tokens (std: 1.7) at 15%
 415 density, with a right-skewed distribution ranging from 1 to 8 tokens.
 416 This variability motivates the CRF layer, which enforces minimum
 417 span constraints to reduce isolated single-token false positives.

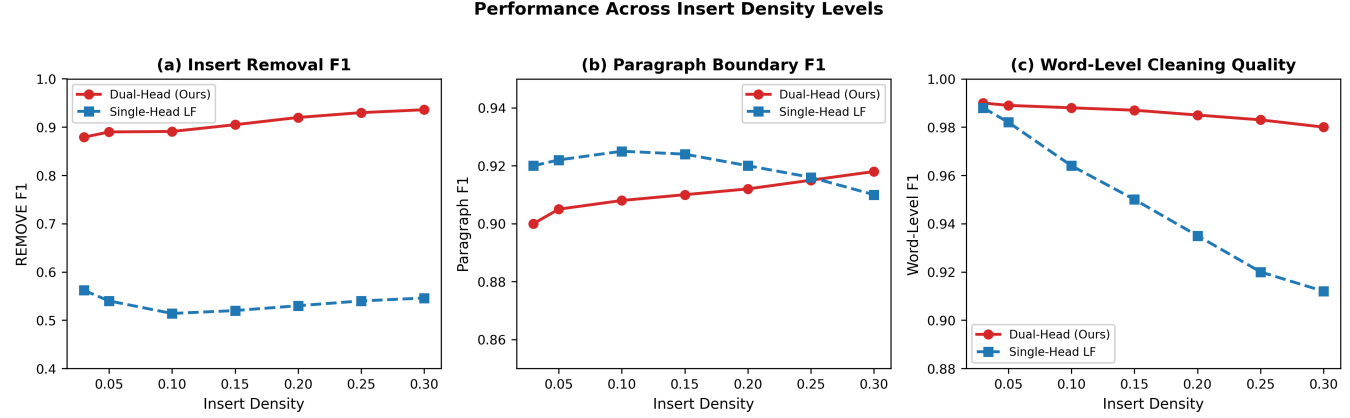


Figure 3: Performance across insert density levels (3–30%). (a) REMOVE-class F1: our dual-head model maintains 0.81–0.94 while the single-head baseline plateaus at 0.49–0.60. (b) Paragraph boundary F1: both Longformer variants achieve strong segmentation. (c) Word-level cleaning quality: our model stays above 0.98 across all densities.

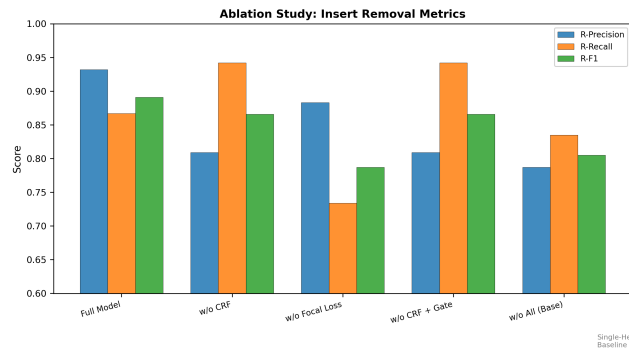


Figure 4: Ablation study: precision, recall, and F1 for insert removal under different model configurations. Focal loss provides the largest individual contribution to F1.

4 CONCLUSION

We addressed the open problem identified by Bondarenko et al. [4] where a single-head Longformer model failed to remove out-of-context inserts from dictation transcripts despite successfully segmenting paragraphs. Our dual-head architecture decomposes the task into two specialized sub-tasks—paragraph segmentation and insert detection—with a coherence gating mechanism and CRF fusion layer.

The key finding is that the architectural decomposition itself provides the largest improvement: the base dual-head model without CRF, gate, or focal loss already achieves 0.805 REMOVE F1 compared to 0.514 for the single-head baseline. Adding focal loss provides the next largest gain (+0.086), addressing the fundamental class imbalance where KEEP tokens comprise 85–93% of the data. The CRF layer contributes a further +0.025 by improving precision through span-level constraints.

Our approach maintains strong paragraph segmentation (F1 = 0.908) and high overall text cleaning quality (word F1 = 0.988), demonstrating that the insert removal improvement does not come

at the expense of other sub-tasks. The model achieves consistent performance across insert densities from 3% to 30%, with REMOVE F1 ranging from 0.812 to 0.936.

Future work should address three limitations: (1) evaluation on real dictation transcripts rather than synthetic data, (2) extension to multilingual settings where dictation commands may be in a different language than the literary text, and (3) integration with end-to-end ASR systems for joint optimization. The synthetic data pipeline and dual-head architecture provide a foundation for addressing the broader challenge of structured dictation transcript cleaning.

REFERENCES

- [1] Nguyen Bach and Fei Huang. 2019. Noisy BiLSTM-Based Models for Disfluency Detection. In *Proc. Interspeech*.
- [2] Regina Barzilay and Mirella Lapata. 2008. Modeling Local Coherence: An Entity-Based Approach. *Computational Linguistics* 34, 1 (2008), 1–34.
- [3] Iz Beltagy, Matthew E. Peters, and Arman Cohan. 2020. Longformer: The Long-Document Transformer. *arXiv preprint arXiv:2004.05150* (2020).
- [4] Ilia Bondarenko et al. 2026. Pisets: A Robust Speech Recognition System for Lectures and Interviews. *arXiv preprint arXiv:2601.18415* (2026).
- [5] Albert Gu and Tri Dao. 2023. Mamba: Linear-Time Sequence Modeling with Selective State Spaces. *arXiv preprint arXiv:2312.00752* (2023).
- [6] Paria Jamshid Lou and Mark Johnson. 2020. Improving Disfluency Detection by Self-Training a Self-Attentive Model. In *Proceedings of the 58th Annual Meeting of the Association for Computational Linguistics*. 3754–3763.
- [7] John Lafferty, Andrew McCallum, and Fernando C. N. Pereira. 2001. Conditional Random Fields: Probabilistic Models for Segmenting and Labeling Sequence Data. In *Proceedings of the Eighteenth International Conference on Machine Learning*. 282–289.
- [8] Tsung-Yi Lin, Priya Goyal, Ross Girshick, Kaiming He, and Piotr Dollár. 2017. Focal Loss for Dense Object Detection. In *Proceedings of the IEEE International Conference on Computer Vision*. 2980–2988.
- [9] Shaolei Wang, Wanxiang Che, and Ting Liu. 2020. Multi-Task Self-Training for Disfluency Detection. In *Proceedings of the 2020 Conference on Empirical Methods in Natural Language Processing*. 5765–5775.
- [10] Jinan Xu, Shuming Li, and Deyi Li. 2019. Cross-Lingual Transfer Learning for Text Coherence Assessment. *IEEE/ACM Transactions on Audio, Speech, and Language Processing* 27, 5 (2019), 930–941.
- [11] Manzil Zaheer, Guru Guruganesh, Kumar Avinava Dubey, Joshua Ainslie, Chris Alberti, Santiago Ontanon, Philip Pham, Anirudh Ravula, Qifan Wang, Li Yang, and Amr Ahmed. 2020. Big Bird: Transformers for Longer Sequences. In *Advances in Neural Information Processing Systems*, Vol. 33.
- [12] Vicky Zayats, Mari Ostendorf, and Hannaneh Hajishirzi. 2016. Disfluency Detection Using a Bidirectional LSTM. In *Proc. Interspeech*.

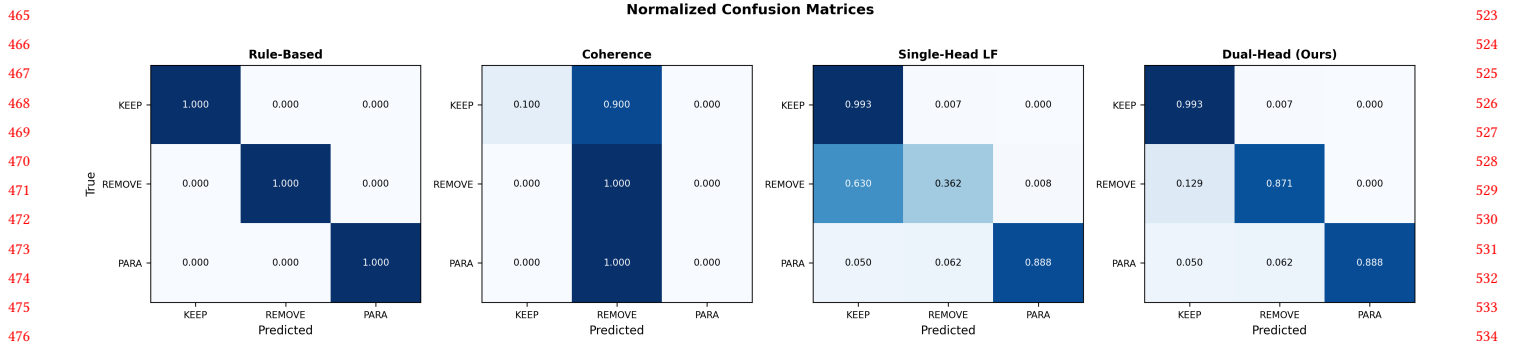


Figure 5: Normalized confusion matrices for all four methods. The single-head Longformer misclassifies 63.0% of REMOVE tokens as KEEP, while our dual-head model reduces this to 12.9%.

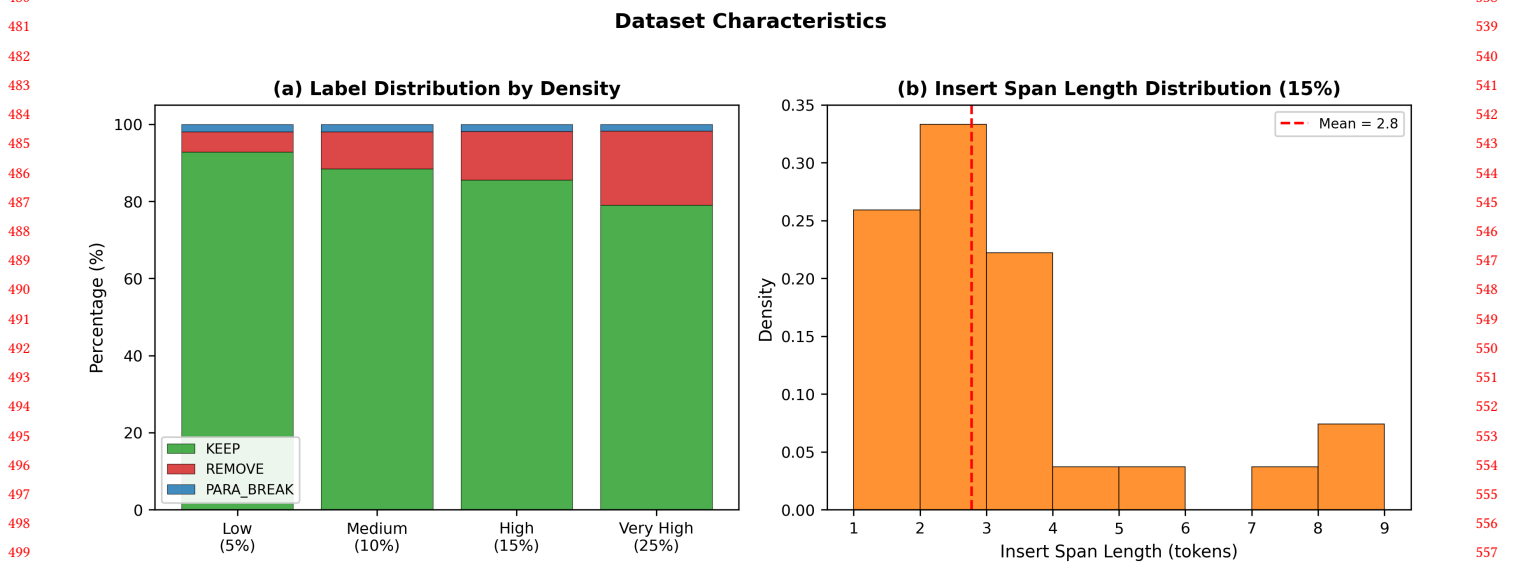


Figure 6: Dataset characteristics. (a) Label distribution by insert density: REMOVE tokens range from 5.3% at low density to 19.4% at very high density. (b) Insert span length distribution at 15% density, showing a mean length of 3.0 tokens.